International Journal of Signal Processing, Image Processing and Pattern Recognition
Vol.9, No.12, (2016), pp.113-122
http://dx.doi.org/10.14257/ijsip.2016.9.12.12

Research on Medical Image Classification and Recognition Based on Multi Feature Fusion

Feng Yingying[1] and Zhou Hongzhi[1]

[1]*College of information Engineering, Fuyang Teachers 'College, Fuyang Anhui 236041, China*
517491038@qq.com

Abstract

In order to prevent the moving vehicle shadows from being wrongly detected as the target, a shadow detection algorithm fusing chromaticity, brightness and edge gradient information is proposed in this paper. Specifically, shadow feature image is established according to the variation proportions of the chromaticity and the brightness of the foreground and the background of the moving target, and then the area with the maximum chromaticity is regarded as the vehicle search start point to gradually absorb the surrounding areas with the richest edge gradient so as to form the vehicle body area, and then remaining area of the foreground not containing the vehicle body is regarded as the shadow candidate area, and then the region growing method is adopted to obtain various shadow sub-areas for integration so as to form the vehicle shadow area. The experiment result shows that this method has the advantages of little manual intervention, high shadow detection rate, etc.

Keywords: *Shadow detection; Region growing; Image division; intelligent transportation*

1. Introduction

In the video analysis of the intelligent transportation system, the vehicle shadow is often wrongly judged as a part of the moving target to cause the adhesion of several moving targets, thus bringing negative influence to such subsequent links as target tracing & recognition and reducing the accuracy of such transportation parameters as vehicle type, vehicle flow rate and vehicle density. Therefore, the accurate shadow detection is an important basis for the video analysis of the intelligent transportation system. In consideration of illumination variation and shadow generation complexity, such method is limited by the generalization ability of the classifiers, *etc.* Under the hypothesis that the local texture, edge, gradient, color and other features of the shadow area are basically unchanged, the method based on shadow attribute mainly aims at fusing several invariant features in such color spaces as HIS, HSV and YUV and meanwhile combining the brightness variation to judge whether the pixel belongs to the shadow area. However, such features as the texture, chromaticity and saturation of the shadow area are usually changed, thus influencing the universality of the method. In order to conquer the above disadvantages, the shadow detection algorithm fusing chromaticity, brightness and edge gradient features is proposed in this paper.

2. Establishment of Shadow Feature Image

Under certain brightness condition, the hues inside and outside the shadow area of the same object are approximately consistent with each other, and only the brightness is changed. According to the shadow model in literature [4], brightness *IB* inside the shadow

ISSN: 2005-4254 IJSIP

area of the same object and brightness *IF* inside the non-shadow area have the following relationship:

$$I_F^Y = \beta I_B^Y, \quad \text{where } \beta = \frac{r+1}{k_i r+1} \tag{1}$$

Where r is the proportion of the direct light and the ambient light and ki is the coefficient in the interval of [0, 1] and represents the irradiation degree of the direct light to the surface of the object. Formula (1) indicates that the shadow can reduce brightness component Y of the object, and the proportion is β.

In the shadow area, the brightness variations of the pixels on the surface of the homogeneous object are approximate to each other, namely: proportions β are approximate to each other. Therefore, in *YCbCr* color space, the variation proportions of the foreground and the background of the moving target are adopted to construct shadow feature image *Ifea*, namely:

$$I_{fea}(x,y) = \frac{\sum_{(x,y)\in D} Y_F(x,y)}{\sum_{(x,y)\in D} Y_B(x,y)} \bullet R_{Cb} \bullet R_{Cr} \tag{2}$$

Where
$$R_{Cb} = 1 + \frac{\left| \sum_{(x,y)\in D} Cb_F(x,y) - \sum_{(x,y)\in D} Cb_B(x,y) \right|}{\sum_{(x,y)\in D} \left[BW(x,y) \bullet Cb_B(x,y) \right]}$$

And
$$R_{Cr} = 1 + \frac{\left| \sum_{(x,y)\in D} Cr_F(x,y) - \sum_{(x,y)\in D} Cr_B(x,y) \right|}{\sum_{(x,y)\in D} \left[BW(x,y) \bullet Cr_B(x,y) \right]}.$$

In Formula (2), factors *RCb* and *RCr* are the proportion values of chromatic aberration *Cb* component and chromatic aberration *Cr* component respectively in foreground *F* and background *B*, and *D* is the neighbor of pixel $P(x, y)$. When brightness *Y* of background image *IB* is zero, in order to avoid zero denominator, brightness *Y* of background image *IB* should be replaced by the mean value of brightness *Y* of neighbor *D*. According to Formula (2), *Ifea* of the area outside the moving target is about 1, and *Ifea* of the vehicle body area inside the moving target is more than or less than 1 along with the change of color and illumination, but *Ifea* of the shadow area is certainly equal to 1.

In the shadow area, brightness decay proportions β of the pixels on the surface of the homogeneous object are approximate to each other, and the chromaticity is only slightly changed, so the pixel values in the shadow area of feature image *Ifea* are approximate to each other, and the original texture of the shadow area is obviously restrained, thus becoming relatively flat. Additionally, in consideration that the brightness and chromaticity variation of the non-shadow area (such as vehicle body) of the moving vehicle target is not proportionally decayed, the non-shadow area of feature image *Ifea* can not only reserve the texture variation of the original brightness component, but also increase the two chromatic aberration factors *RCb* and *RCr* along with the change of the vehicle body color, thus to further strengthen the texture of the non-shadow area of feature image *Ifea*. The moving target with shadow is as shown in Figure 1(a), and the background image is as shown in Figure 1(b), and the feature image of the moving target constructed according to Formula (2) is as shown in Figure 1(c). As shown in Figure 1(c),

the zebra stripes, the road signs and other textures in the shadow area are obviously weakened.

(a) Moving Target (b) Background Image (c) Feature Image *Ifea*

Figure 1. Feature Image *Ifea*

The texture of the shadow area in feature image *Ifea* is weakened but the texture of the vehicle body is well reserved, so Sobel operator is adopted to extract edge gradient image *Iedge* according to Formula (3), wherein the shadow area includes less edge information but the vehicle body area includes rich edge information.

$$I_{edge}(x,y)=(G_x+G_y)\bullet\frac{\sum_{(x,y)\in D}Cb_F(x,y)}{\sum_{(x,y)\in D}Cb_B(x,y)}\bullet\frac{\sum_{(x,y)\in D}Cr_F(x,y)}{\sum_{(x,y)\in D}Cr_B(x,y)} \tag{3}$$

Where
$$G_x=I_{fea}(x-1,y-1)+2I_{fea}(x,y-1)+I_{fea}(x+1,y-1)$$
$$-I_{fea}(x-1,y+1)-2I_{fea}(x,y+1)+I_{fea}(x+1,y+1),$$

and
$$G_y=I_{fea}(x-1,y-1)+2I_{fea}(x-1,y)+I_{fea}(x-1,y+1)$$
$$-I_{fea}(x+1,y-1)-2I_{fea}(x+1,y)-I_{fea}(x+1,y+1).$$

In order to reduce the influence of the fine edge gradient, the maximum between-cluster variance is adopted to respectively find threshold value *Tfea* of feature image *Ifea* and threshold value *Tedge* of edge gradient image *Iedge*, and then feature image *Ifea* and edge gradient image *Iedge* are fused according to Formula (4) to form new feature image *M*, as shown in Figure 2.

$$M(x,y)=I_{edge}+I_{fea}(x,y) \tag{4}$$

$$I_{edge}(x,y)=\begin{cases}I_{edge}(x,y) & I_{edge}(x,y)\geq T_{edge}\\ 0 & I_{edge}(x,y)<T_{edge}\end{cases}$$

Where
$$I_{fea}(x,y)=\begin{cases}I_{fea}(x,y) & I_{fea}(x,y)\geq T_{fea}\\ 0 & I_{fea}(x,y)<T_{fea}\end{cases}$$ and.

Figure 2. Feature Image M Fused with Brightness, Chromaticity and Edge Information

3. Judgment of Shadow Direction

Due to the existence of the shadows, the area of the moving target is expanded to make the centroid of the binary foreground image *BW* more partial to the shadow area. If the centroid is set as *C* (*xc*, *yc*), then the following formula can be obtained:

$$y_c = \frac{1}{n}\sum_{i=1}^{m}\sum_{j=1}^{n} j \cdot BW(i, j) \tag{5}$$

According to the gray level distribution characteristics of feature image *M*, the feature points of the shadow area are sparsely distributed while those of the vehicle body are intensively distributed, so the centroid of feature image *M* is more close to the vehicle body. If the mass center is set as *Z* (*xz*, *yz*), then the following formula can be obtained:

$$x_z = \frac{1}{n}\sum_{i=1}^{m}\sum_{j=1}^{n} i \cdot M(i, j) \cdot BW(i, j)$$

$$y_z = \frac{1}{n}\sum_{i=1}^{m}\sum_{j=1}^{n} j \cdot M(i, j) \cdot BW(i, j) \tag{6}$$

Where $n = \sum_{i=1}^{m}\sum_{j=1}^{n} BW(i, j)$

According to the analysis of the positions of *C* (*xc*, *yc*) and *Z* (*xz*, *yz*), we can judge the direction of the shadow. Therefore, the mask image as shown in Figure 3 is designed.

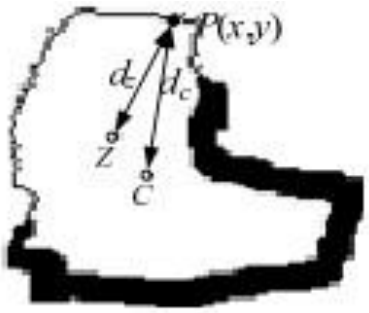

Figure 3. Mass Center, Centroid and Shadow Direction of Feature Image M

In the mask image, the shadow area has thick boundary while the non-shadow area has thin boundary. Specifically, the boundary width is set as *L*, *P(x, y)* is a point at boundary *B* of binary foreground image *BW*, *dC* is the distance from *P(x, y)* to centroid *C*, and *dZ* is the distance from *P(x, y)* to mass center *Z*. Then, boundary width *L* can be calculated according to Formula (7).

$$L = \lambda \cdot arc\cot\left[\alpha \cdot (d_c - d_z)\right] \tag{7}$$

Where λ is the amplitude adjustment factor, α is the variation rate adjustment factor, and *L* is the round-off integer. If *dC*>*dZ* is true, then it is indicated that *P(x, y)* is at the vehicle body side and *L* value is relatively small; if *dC*<*dZ* is true, then it is indicated that *P(x, y)* is at the shadow side and *L* value is relatively large.

Subsequently, the mask image is applied to feature image *M* to make the values of the pixels covered by the mask image in feature image *M* as zero. The mask image is wide in the shadow area but narrow in the non-shadow area, thus to not only well restrain the

boundary information of the shadow area and the background, but also reserve the edge information of the vehicle body.

4. Selection of Shadow Candidate Area

Mean shift algorithm is adopted in this paper to segment feature image *Ifea* to obtain *N* sub-areas and form set *Dseg*(N). Area *Dseg*(*i*) in foreground image *IF*, calculated to have the maximum difference with the background image in the aspects of chromaticity *Cb* and *Cr* components according to Formula (8), is regarded as the search start area of the vehicle body, as shown in Figure 4. Therein, the area with the darkest color is namely search start area *Dseg*(*i*).

$$D_{seg}(i) = \arg\max_{F}\left[\sum_{(x,y)\in D_{seg}}\left(\left|Cb_F(x,y)-Cb_B(x,y)\right|+\left|Cr_F(x,y)-Cr_B(x,y)\right|\right)\right] \quad (8)$$

In order to search the vehicle body area, it is necessary to firstly obtain boundary *b* of search start area *Dseg*(i) and find *r* areas connected to *Dseg*(*i*) along boundary *b* to form set [*Dseg*(*1*), *Dseg*(*2*)…*Dseg*(*r*)], and then take area *Dseg*(*j*) containing feature image *M* with the maximum mean value in the set, and then combine it with *Dseg*(*i*) to obtain larger area *Dseg*(*i*), namely:

$$D_{seg}^{k}(i) = D_{seg}^{k-1}(i) + D_{seg}^{k-1}(j) \quad (9)$$

Where $D_{seg}^{k-1}(j) = \arg\max_{m=0,1..r}\left\{\frac{1}{n}\sum_{(x,y)\in D_{seg}(m)} M(x,y)\right\}$, *n* is the total number of the pixels in area *Dseg*(*i*), and *k* is the present iteration count.

Then, area *Dseg*(*i*) is obtained through loop iteration till the iteration termination condition Formula (10) is met. Namely: *Dseg*(*i*) iteration should be terminated when the mean feature value of other sub-areas neighboring to area *Dseg*(*i*) in feature image *M*. Threshold value ξ is the dimensionless approximate to zero and should be set according to actual conditions.

$$\max\left\{\frac{1}{n}\sum_{(x,y)\in D_{seg}(m)} M(x,y)\right\} < \xi \quad m = r+1, r+2 \ldots r+k \quad (10)$$

Other sub-areas not contacting area *Dseg*(*i*) form two sets: $Q_1 = \left[D_{seg}(r+1), D_{seg}(r+2)\ldots D_{seg}(r+k)\right]$ and $Q_2 = \left[D_{seg}(r+k+1), D_{seg}(r+k+2)\ldots D_{seg}(N)\right]$, wherein *Q1* is the set of the surrounding sub-areas neighboring to *Dseg*(i) and *Q2* is the set of the surrounding sub-areas not neighboring to *Dseg*(i).

If *Q1* and *Q2* are both empty sets, then it is indicated that the moving target does not have any shadow. If the mean feature value of the area in set *Q2* is more than threshold value ξ, then it is indicated that multiple moving targets are adhered together. In such case, the shadow analysis should be carried out for another target for set *Q2* according to Formula (9), and the iteration should be terminated to obtain new set *Q2* till Formula (10) can be met. Finally, all elements of sets *Q1* and *Q2* should be taken as the shadow candidate area.

Figure 4. Search Start Point and Shadow Candidate Area of Vehicle Body

In Figure 4, sets *Q1* and *Q2* are not empty, thus indicating that the moving target has shadows. After iteration termination, *Dseg*(*i*) is the vehicle body part, namely the gray area shown in Figure 4, and the blank area is the shadow candidate area.

5. Detection of Shadow Area

Among the elements [*Dseg*(*r+1*), *Dseg*(*r+2*)…*Dseg*(*N*)] in sets *Q1* and *Q2*, area *Dseg*(*i*) is taken as the start point, and the region growing method is adopted to search shadow sub-area *S*(*j*) in feature image *Ifea*(*x, y*). *S*(*j*) is a binary image, wherein the value of the pixels meeting the following growing criterion is 1 while the value of the pixels not meeting the following growing criterion is 0. The criterion of the region growing method is as follows:

$$S(j)=\left\{P(x,y):M(x,y)<T_{edge}\ \&\left|I_{fea}(x,y)-I_{fea}(x+d,y+d)\right|<\xi\sigma\ \&\ BW(x,y)=1\right\} \quad (11)$$

Where *Ifea*(*x, y*) is the value of the present search point *P*(*x, y*), *Ifea*(*x+d, y+d*) is the value of the next four-neighbor search start point, *Tedge* is the threshold value obtained through the maximum between-cluster variance method for edge image *Iedge*, ξ is the adjustment factor, σ is the variance of all pixels of feature image *Ifea* in set [*Dseg*(*r+1*), *Dseg*(*r+2*)…*Dseg*(*N*)] .

It is necessary to start from the sub-area represented by each element of sets *Q1* and *Q2*, and traverse the sub-area and the surrounding area thereof to obtain shadow sub-areas *S(r+1)*, *S*(*r+2*)…*S*(*N*) so as to obtain all shadow areas S of the moving vehicle through the logic "OR" operation of all shadow sub-areas, namely:

$$S=D_{seg}(r+1)\left|D_{seg}(r+2)\right|\ldots D_{seg}(N)\left|S(r+1)\right|S(r+2)\left|\ldots S(N)\right.$$

6. Shadow Detection Algorithm Flow

(1) The moving target detection is the first step of the moving vehicle shadow detection. In this paper, *PBAS* algorithm is selected to extract the background and the motion foreground, wherein *PBAS* algorithm integrates the advantages of *SACON* and *VIBE* algorithms and is also improved, and the background modeling thereof is similar to that of *SACON* algorithm, namely: the first *N* frames of pixels and the gradient magnitude are integrated to establish the background model. Additionally, compared with *VIBE* algorithm in the aspects of background update and foreground detection, *PBAS* algorithm has adaptive update rate, and the neighbor pixel value rather than the pixel value thereof is adopted for updating.

(2) Feature image *M* fused with brightness, chromaticity and edge gradient information is obtained in *YCbCr* color space.

(3) After the mean shift algorithm is adopted to segment feature image *M*, the area having maximum chromaticity difference with the background is regarded as search start area *Dseg*(*i*) of the vehicle body.

(4) Afterwards, it is necessary to start from search start area *Dseg*(*i*) and find *r* areas connected to *Dseg*(*i*), and select area *Dseg*(*j*) with the maximum mean feature value in feature image *M*, and combine it with area *Dseg*(*i*) so as to obtain larger area *Dseg*(*i*).

(5) Among all areas connected to area *Dseg*(*i*), if there is any area which cannot meet Formula (10), then it is necessary to return to Step (4); or else, other sub-areas not contacting area *Dseg*(*i*) should form two sets *Q1* and *Q2*. If the mean feature value of the area in set *Q2* is more than threshold value ξ, then it is indicated that multiple moving targets are adhered to each other, and it is necessary to return to Step (4).

(6) Finally, it is necessary to start from the sub-area represented by each element of sets *Q1* and *Q2*, and adopt the region growing method to traverse shadow sub-areas *S*(*r+1*), *S*(*r+2*)…*S*(*N*) in feature image *Ifea*(*x, y*) so as to obtain all shadow areas ξ of the moving vehicle through the logic "OR" operation of all shadow sub-areas.

7. Experiment Result and Analysis

The programming environment of the experiment in this paper is VS2010 and Opencv2.0, and PC configuration is as follows: CPU Core i5-4590, dominant frequency 3.3GHz, memory 4GB, and operating system Win7. Video sequence mv2_ 001 and the monitoring video sequence for a certain highway in literature [16] are selected for the experiment, wherein the resolution ratio of each frame of the video is 640 X 480 pixels. After background modeling and foreground detection, the source code of LR Textures algorithm in literature [17] is adopted for the comparison experiment. The experiment results of the five representative frames are as shown in Figure 5.

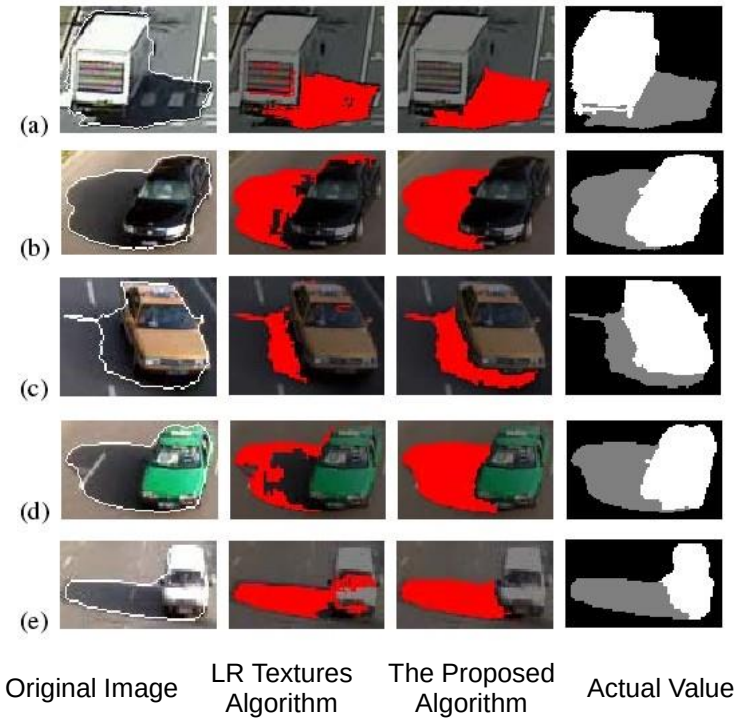

Figure 5. Shadow Detection Result

According to Figure 5, for LR textures algorithm, some shadow areas are missed, and the shadow has holes, and some pixels of the moving target can be easily wrongly judged as shadow, such as the glass and tyre areas of the vehicle. In contrast, the shadow detected by the proposed algorithm has fewer holes and completely reserves the moving target, and the proposed algorithm can well distinguish the shadow and the moving target, thus having better effect and higher accuracy.

For the quantitative evaluation of the experiment results, shadow detection rate η and shadow resolution ratio ξ mentioned in literature [17] are adopted as the evaluation index. The larger values of the two indexes indicate better shadow detection effect. The result for the quantitative comparison with LR Textures algorithm in literature [17] is as shown in Table 1.

Table 1. Quantitative Evaluation Result

Video	Detection Rate η		Resolution Ratio ξ	
	LR Textures		LR Textures	
	LR Textures	The Proposed Algorithm	LR Textures	The Proposed Algorithm
a	0.7702	0.9087	0.9243	0.9910
b	0.8249	0.9914	0.9434	0.9638
c	0.5919	0.9798	0.9875	0.9587
d	0.4984	0.9775	0.9770	0.9742
e	0.7352	0.9368	0.7308	0.9956

The comparison result shows: in LR Textures algorithm, some shadow points are wrongly detected as the target points and *FNs* extracted thereby is relatively large, thus making shadow detection rate η relatively small; for the proposed algorithm, shadow detection rate η is obviously higher than the result in literature [17], thus indicating that the proposed algorithm is superior to LR Textures algorithm in literature [17] in the aspect of shadow detection effect. In the aspect of shadow resolution ration ξ, the two algorithms have the similar results for videos (a) ~ (d), but the glass and license plate areas of the vehicle are wrongly detected by LR Textures algorithm as the moving target in video (e) and FNs extracted thereby is relatively large, thus resulting in small shadow resolution ratio ξ, namely 0.7308, which is obviously less than the experiment result of the proposed algorithm. Therefore, the proposed algorithm is superior to LR Textures algorithm in literature [17].

8. Conclusion

On the basis of background modeling and foreground detection, such feature information as chromaticity, brightness and gradient are fused to establish the feature image for shadow detection. Specifically, the distribution features of the centroid and the mass center of the edge gradient image are adopted to construct the mask image to restrain the edge information of the shadow area and the background area in the feature image. After the mean shift algorithm is adopted for image segmentation, the area with maximum chromaticity difference is regarded as the vehicle body search start point to subsequently gradually absorb the surrounding area with maximum edge gradient so as to form the vehicle body area.

Acknowledgements

Anhui natural science research project“Dynamic perspectives of moving target tracking theory and method research based on computer vision”, project number: (2015FXSK02), Anhui natural science research project“Big data environment video text access to key technology research”, project number: (2015FXSK03); Anhui natural science research project “Moving target localization and tracking technology research under the complex visual scene based on multi-camera coordination”, project number: (KJ2016A554); Anhui natural science research project“The phase space reconstruction and prediction model of network public opinion support vector machine (SVM)”, project number: (KJ2016A556).

References

[1] T. Su, W. Wang and Z. Lv, “Rapid Delaunay triangulation for randomly distributed point cloud data using adaptive Hilbert curve”, Computers & Graphics, vol. 54, **(2016)**, pp. 65-74.
[2] J. Hu, Z. Gao and W. Pan, “Multiangle Social Network Recommendation Algorithms and Similarity Network Evaluation”, Journal of Applied Mathematics, 2013, **(2013)**.
[3] S. Zhou, L. Mi, H. Chen and Y. Geng, “Building detection in Digital surface model”, 2013 IEEE International Conference on Imaging Systems and Techniques (IST), **(2012)** Oct.
[4] J. He, Y. Geng and K. Pahlavan, “Toward Accurate Human Tracking: Modeling Time-of-Arrival for Wireless Wearable Sensors in Multipath Environment”, IEEE Sensor Journal, vol. 14, no. 11, **(2014)** Nov., pp. 3996-4006.
[5] Z. Lv, A. Halawani and S. Fen, “Touch-less Interactive Augmented Reality Game on Vision Based Wearable Device”, Personal and Ubiquitous Computing, vol. 19, no. 3, **(2015)**, pp. 551-567.
[6] G. Bao, L. Mi, Y. Geng, M. Zhou and K. Pahlavan, “A video-based speed estimation technique for localizing the wireless capsule endoscope inside gastrointestinal tract”, 2014 36th Annual International Conference of the IEEE Engineering in Medicine and Biology Society (EMBC), **(2014)** Aug.
[7] D. Zeng and Y. Geng, “Content distribution mechanism in mobile P2P network”, Journal of Networks, vol. 9, no. 5, **(2014)** Jan., pp. 1229-1236.
[8] W. Gu, Z. Lv and M. Hao, “Change detection method for remote sensing images based on an improved Markov random field”, Multimedia Tools and Applications, **(2015)**, pp. 1-16.
[9] J. Hu and Z. Gao, “Modules identification in gene positive networks of hepatocellular carcinoma using Pearson agglomerative method and Pearson cohesion coupling modularity”, Journal of Applied Mathematics, 2012, **(2012)**.
[10] Y. Geng, J. Chen, R. Fu, G. Bao and K. Pahlavan, “Enlighten Wearable Physiological Monitoring systems”, On-Body RF Characteristics Based Human Motion Classification Using a Support Vector Machine, vol.99, **(2015)**, pp. 1-16.
[11] X. Song and Y. Geng, “Distributed Community Detection Optimization Algorithm for Complex Networks”, Journal of Networks, vol. 9, no. 10, **(2014)**, pp. 2758-2765.
[12] K. Pahlavan, P. Krishnamurthy and Y. Geng, “Localization Challenges for the Emergence of the Smart World”, Access, IEEE, vol. 3, no. 1, **(2015)**, pp. 1-11.
[13] J. He, Y. Geng, Y. Wan, S. Li and K. Pahlavan, “A cyber physical test-bed for virtualization of RF access environment for body sensor network”, Sensors Journal, IEEE, vol. 13, no. 10, **(2013)**, pp. 3826-3836.
[14] Z. Lv, A. Tek and F. Da Silva, “Game on, science-how video game technology may help biologists tackle visualization challenges”, PloS one, vol. 8, no. 3, **(2013)**, pp. 57990.

Authors

Feng Yingying, received her M.S. degree in computer application of professional engineering from China university of geosciences, in Wuhan, China. She is currently an associate professor in fuyang normal college information engineering college. Her research interest is mainly in the area of computer software, wireless sensor and image processing. She has published several research papers in scholarly journals in the above research areas and has won two national utility model patents.